Determination of the Platinum and Ruthenium Surface Areas in Platinum−Ruthenium Alloy Electrocatalysts by Underpotential Deposition of Copper. I. Unsupported Catalysts

Clare L. Green and Anthony Kucernak*

Department of Chemistry, Imperial College of Science Technology and Medicine, London SW7 2AY, U.K.

Received: August 17, 2001; In Final Form: November 2, 2001

Underpotential deposition (upd) of copper has been used to characterize platinum, ruthenium, and platinum−ruthenium high-surface-area unsupported (powder black) electrocatalysts. The surface areas thus obtained compare favorably with those determined by the more conventional electrochemical methods of monolayer CO and hydrogen oxidation. The differing adsorption energies for Cu on either Pt or Ru allow the peaks for upd copper deposited on alloy Pt−Ru to be resolved into their constituent components. Thus, in addition to the surface area, the surface composition of the Pt−Ru electrocatalyst can be determined. This approach distinguishes between bare ruthenium (i.e., metallic) and oxidized ruthenium sites as the upd copper does not deposit on the latter. The ruthenium surface area is found to remain high up to 0.45 V (vs RHE) and then to fall linearly with potential. Polarization at high potentials [1.45 V (vs RHE)] leaves a material in which metallic ruthenium cannot be recovered by electrochemical reduction. This is caused by oxidation of the ruthenium to a state that either dissolves in the aqueous phase and is lost or produces a form of oxidized ruthenium that is in a state that cannot be electrochemically reduced.

Introduction

Platinum alloy electrocatalysts have found great favor for use in both solid polymer and phosphoric acid fuel cells (SPFCs and PAFCs, respectively). Specifically, such fuel cells are often required to run on either reformate (a mixture of hydrogen and carbon monoxide) or methanol (i.e., the direct methanol fuel cell, DMFC). In these cases, the presence of a second (or more) alloying component in addition to the platinum offers improved performance by facilitating the removal of intermediates that are adsorbed on the catalyst surface. The presence of an alloying component can alter the activity of a catalyst through either electronic effects or a "bifunctional" mechanism in which each alloy component either is active for removal of an intermediate or allows the adsorption of a reactive species that facilitates the overall reaction on the catalyst. An example of the former is the suggested effect on the oxygen reduction activity of a class of catalysts produced using a "skin" of platinum over an alloy.[1,2] An example of the latter is the Pt−Ru catalyst used in reformate-tolerant fuel cells and the DMFC within which it has been come to be believed that the ruthenium component is active for the adsorption of water—an important component required for the overall oxidation of the carbonaceous species adsorbed on the electrode surface.[3] Obviously, the chemical state and surface composition of these catalysts are important parameters in understanding their activity.

Considering the platinum−ruthenium alloy system, much discussion in the literature has focused on the role of ruthenium metal, oxides and hydrous oxides in the promotion of methanol oxidation in DMFCs.[4−6,] Ruthenium present within Pt−Ru catalysts can exist as either the native metal, an electron- and proton-conducting hydrous oxide (denoted as either RuO_xH_y or $RuO_2{\cdot}xH_2O$) or an insulating, dehydrated oxide (RuO_2).

It is well-known that ruthenium promotes water adsorption and dissociation (eq 2), a key step in the electrooxidation of organic molecules, and hence lowers the onset potential of such oxidations in comparison with Pt alone. For instance, below is the presumed predominant pathway for the oxidation of CO on Pt−Ru alloy

$$CO + Pt_{surf} \rightarrow Pt_{surf}CO \quad (1)$$

$$Ru_{surf} + H_2O \rightarrow Ru_{surf}OH + H^+ + e^- \quad (2)$$

$$Ru_{surf}OH + Pt_{surf}CO \rightarrow Ru_{surf} + Pt_{surf} + CO_2 + H^+ + e^- \quad (3)$$

where the subscript surf indicates that we are dealing with metal atoms on the surface of a bulk metal catalyst. Providing that $\theta_{Ru} > 0$, where θ_{Ru} is the surface coverage of ruthenium on the catalyst, the peak potential for CO oxidation shifts from the Pt-only value of 0.7 to 0.5 V (vs RHE).[7]

For comparisons to be made between the intrinsic activities of different catalysts, measurements of the true surface areas of high-surface-area catalysts are required. Using electrode dimensions and catalyst loadings, along with the known specific surface area of the catalyst (determined, for instance, using BET measurements), is an unsatisfactory approach as each preparation method results in a different distribution of catalytic particles not all of which will be in contact with both electrolyte and current collector. Furthermore, few methods are available that can accurately provide in situ surface area measurements.

Traditionally, the so-called electrochemical surface area of Pt electrodes has been determined by cyclic voltammetry in an aqueous acidic medium. As each surface platinum atom has the capacity to adsorb close to one hydrogen atom (with some dependency on crystal face), the charge associated with hydrogen adsorption and desorption (eq 4)[8] indicates the number of surface platinum atoms and hence the surface area.

$$Pt + H^+ + e^- \rightarrow Pt{-}H \qquad 210\ \mu C\ cm^{-2} \quad (4)$$

* Author to whom correspondence should be addressed. Phone: +44 20 75945831. Fax: +44 20 75945804. E-mail: a.kucernak@ic.ac.uk

10.1021/jp0131931 CCC: $22.00 © 2002 American Chemical Society
Published on Web 01/09/2002

The accepted value of 210 μC cm^{-2} is an average value for the charge associated with monolayer formation of hydrogen atoms on a polycrystalline platinum surface. However, as alluded to above, the value on individual crystal faces can be quite different, for instance, 150 and 208 μC cm^{-2} for Pt(110) and Pt(100), respectively.[9]

Hydrogen adsorption and stripping is an unsuitable method for the characterization of Ru-containing catalysts because of the overlap of the hydrogen and ruthenium oxidation currents, with the latter commencing at around 0.25 V vs NHE.[10] In addition, seemingly more than one monolayer of hydrogen can be established at a ruthenium surface due to absorption into the oxide lattice as a result of the formation of ruthenium bronzes and also dissolution of atomic hydrogen into the metallic ruthenium (eq 5).

$$\mathrm{Ru} + n\mathrm{H}^+ + n\mathrm{e}^- \rightarrow \mathrm{RuH}_n \qquad (5)$$

CO stripping voltammetry is currently the favored method for measuring the electrochemical surface area of Pt and Ru mono- and bimetallic electrodes.[11] From studies of carefully alloyed catalysts, it has been found that the stripping voltammograms of CO adsorbed on Pt−Ru alloys show a peak potential that shifts depending on the amount of surface Ru present.[12] Gottesfeld et al.[13] proposed this technique as a means of studying surface composition. The peak potential was found to be at a minimum with $\theta_{Ru} = 0.5$ and to increase for both Pt- and Ru-rich surfaces. However, it is unclear as to whether CO is truly a good probe of the Ru surface. Because of the number of possible modes of adsorption onto both Pt and Ru, interpreting the charges attained during the stripping process is difficult. It is generally agreed that CO adsorbs on Pt in a 1:1 linearly bonded fashion. With ruthenium, the situation is more ambiguous, with both linearly bonded and bridge-bonded CO observed. Surprisingly, some researchers suggest that the ratio of CO to ruthenium under certain circumstances can be as high as 2:1.[14] Whether this transcribes well to Pt−Ru alloy systems is unknown, although most researchers assume a 1:1 ratio for this alloy.

Although the bulk composition of alloy catalysts can be easily determined through standard analytical techniques, a further complication arises as a result of surface segregation, the strong enrichment of the surface by one component of a metal alloy, usually the component with the lower heat of sublimation. In the case of a Pt−Ru alloy, it is the platinum that segregates.[15] Gasteiger et al.[16] found that, for a Pt−Ru alloy with a bulk composition of 70.2% platinum, surface enrichment led to an annealed surface composition of 92.1% Pt. It therefore seems very unlikely that there is one numerical conversion factor for determining the electrochemical surface area of all possible catalysts by CO or H adsorption and stripping.

Previously, combinations of spectroscopic techniques such as XPS (X-ray photoelectron spectroscopy), LEISS (low-energy ion-scattering spectroscopy), and AES (Auger electron spectroscopy) have been used to determine the surface area of electrocatalysts;[17,18] however, these techniques require special ultrahigh-vacuum equipment and provide no indication of the catalyst surface that is present under operating conditions.

A nondestructive simple electrochemical technique for the determination of surface area that can easily be applied to the electrode before or after use is required. Such a technique that has previously been applied to both bulk Pt and Ru electrodes is the underpotential deposition (upd) of copper.[19,20] This technique has also been used to characterize the surface of Pt−Pd alloy electrodes.[21]

Underpotential deposition is the deposition of metal atoms onto an electrode surface in mono- or submonolayer quantities at potentials more positive than those required for bulk deposition. Several review articles are available that examine the subject in depth.[22−25]

Copper is an ideal metal for upd on both platinum and ruthenium because of the similarity of the atomic radii of the three metals—Cu, 0.128 nm; Pt, 0.1385 nm; and Ru, 0.134 nm. Integration of the peak area corresponding to upd stripping allows the surface area to be calculated with the assumption of an adsorption ratio of a single Cu atom to each surface metal atom and an electrosorption valency of +2.[26]

$$\mathrm{Cu}_{\mathrm{upd}} \rightarrow \mathrm{Cu}^{2+} + 2\mathrm{e}^- \qquad 420\ \mu\mathrm{C\ cm}^{-2} \qquad (6)$$

In this paper, we initially consider the copper upd process on planar platinum and ruthenium electrodes and show that it is possible to deposit copper at monolayer coverage by judicious choice of electrochemical potential and deposition time. Next, we show that the results obtained on high-surface-area platinum, ruthenium, and platinum−ruthenium powders are equivalent to those seen on the planar electrodes and that the surface areas calculated agree with those obtained via other means. Finally, we use the unique property of the copper upd process, namely, that we can distinguish whether the copper is being deposited on platinum or ruthenium sites to allow us to determine the surface coverage of metallic ruthenium on the surface of a high-surface-area platinum−ruthenium black. We use this information to gain valuable insights into the structure of platinum−ruthenium catalysts operating under fuel-cell-like conditions.

Experimental Section

Solutions were prepared from 98% H_2SO_4 (BDH AnalaR grade) and $CuSO_4 \cdot 5H_2O$ (BDH AnalaR cupric sulfate) with deionized water (18 MΩ cm^{-1} conductance, Millipore MilliQ system) and were degassed using oxygen-free nitrogen (BOC Gases, 99.998%).

Preparation of High-Surface-Area Metal Black Electrodes. The high-surface-area powder blacks were obtained from Johnson-Matthey Plc. The platinum−ruthenium black had an analyzed bulk composition of 58.5 wt % Pt and 36.2 wt % Ru, with the remainder being predominantly oxygen. The catalysts were reduced in a flowing H_2/N_2 mixture containing 50 vol % hydrogen at 200 °C for 30 min and cooled under a continuous gas flow. Glassy carbon electrodes (GCEs) were manufactured from rods (5 mm diameter, Sigadur G, Hochtemperatur Werkstoffe GmBH, Thierhaupten, Germany) by sealing in epoxy resin (Buehler). Electrodes were then prepared by evaporating a drop of catalyst solution onto a glassy carbon electrode polished to 1 μm with alumina (Agar Scientific). The catalyst solutions comprised aqueous Nafion solution (5 wt % Nafion, Solution Technologies) and powder black and were diluted with dimethyl formamide (BDH AnalaR) and water to allow for the production of thin films in the region of 1.5−3 μm thick. The target loading of the catalyst was 0.5 mg cm^{-2}. The electrodes were subsequently heat treated at 140 °C to anneal the Nafion, resulting in stable and durable electrodes. The electrodes were wetted with a 2-propanol/water solution (1:10) and washed in water prior to experiments.

Electrochemical Measurements. Electrochemical experiments were performed in a thermostated three-compartment glass cell with a luggin capillary arrangement and a platinum flag counter electrode. A saturated calomel electrode (SCE), carefully protected to eliminate chloride leaks, was used as the

reference electrode, with potentials corrected to the RHE scale, with reference to which all potentials in this paper are quoted. The potentiostat used was an Autolab PSTAT 30 (EcoChemie, Utrecht, The Netherlands), with an FI20 current integration module.

Measurements on bulk polycrystalline Pt were performed on a Pt disk electrode with a diameter of 7 mm polished using an Oxford Electrode rotating polishing system with various grades of alumina terminating in 0.3-μm powder. Following sonication in methanol and immediately before any experiments, the electrode was cycled as described below.

The bulk ruthenium electrodes were produced on 0.127-mm-diameter Ti wire substrates (Aldrich, 99.97%) utilizing a proprietary ruthenium electroless deposition bath containing aqueous $[Ru(NH_3)_6]^{3+}$ and a reducing agent (Johnson-Matthey Plc). The deposits showed low surface roughness and good adherence to the underlying titanium.

Electrodes were cycled in 0.1 mol dm^{-3} H_2SO_4 before each experiment between potential limits of 1.05 and 0.05 V (Ru and Pt−Ru) or 1.45 and 0.05 V (Pt) until the voltammograms did not evolve.

The charges corresponding to the processes of interest (CO oxidation, Cu stripping) were found by subtraction of the scan in background electrolyte alone and integration of the current−voltage curve between the relevant limits.

CO Stripping Voltammetry. Electrodes were electrochemically cleaned in N_2-degassed 0.1 mol dm^{-3} H_2SO_4 as mentioned above, and the potential then held at 0.3 V. Carbon monoxide (99.97%, BOC) was bubbled through the 0.1 mol dm^{-3} H_2SO_4 electrolyte with the electrode held at 0.3 V for 300 s. The solution was then degassed under continued potential control for an additional 600 s before a linear voltammetric scan was initiated from 0.3 V to a potential of 1.3 V for Pt and 1.05 for Ru and Pt−Ru at a scan rate of 0.01 V s^{-1}.

Cu upd Experiments. All copper upd experiments were carried out in a 0.1 mol dm^{-3} H_2SO_4 and 0.002 mol dm^{-3} $CuSO_4$ solution unless otherwise stated. After electrochemical cleaning and transfer into solution containing dissolved cupric ions, the electrodes were polarized at 0.3 V for 60 or 100 s. A linear voltammetric scan was then performed from the admission potential to a point at which all of the upd copper had been oxidized at a scan rate of either 0.002 or 0.01 V s^{-1}. Charges obtained for copper stripping were corrected for the charge associated with any oxide growth (or other background process) by subtracting the charge obtained for the same electrode under the same conditions in the absence of any cupric ions in solution.

Results and Discussion

(a) Effect of Deposition Time and Potential on the Extent of Copper upd Layers. As has been described in the Introduction, copper upd on both Pt and Ru planar electrodes has been previously studied by several workers.[19,20] Displayed in Figure 1 is the cyclic voltammogram of a polycrystalline platinum electrode in a solution composed of 0.1 mol dm^{-3} H_2SO_4 and 0.5×10^{-3} mol dm^{-3} $CuSO_4$ at a scan rate of 0.01 V s^{-1}. For comparison, a voltammogram of the same electrode in the absence of copper is also shown. The hydrogen adsorption region is masked in the presence of copper, and the oxide reduction peak is distorted because of the onset of copper upd. The voltammogram is dominated by the deposition and stripping of both bulk and underpotential-deposited copper. Peak I_C represents the growth of bulk copper on the electrode surface, with the removal of that copper occurring at I_A. Danilov et al. were able to distinguish sites of different adsorption energies

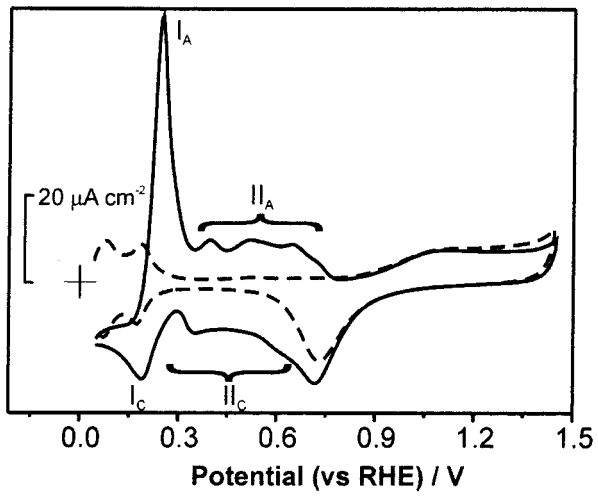

Figure 1. Cyclic voltammogram of a planar bulk Pt electrode in a solution of 0.1 mol dm^{-3} H_2SO_4 and 0.5×10^{-3} mol dm^{-3} $CuSO_4$ at $\nu = 0.01$ V s^{-1}. The voltammogram displays features due to bulk copper stripping and deposition (I_A/I_C) and the underpotential stripping and deposition processes (II_A/II_C).

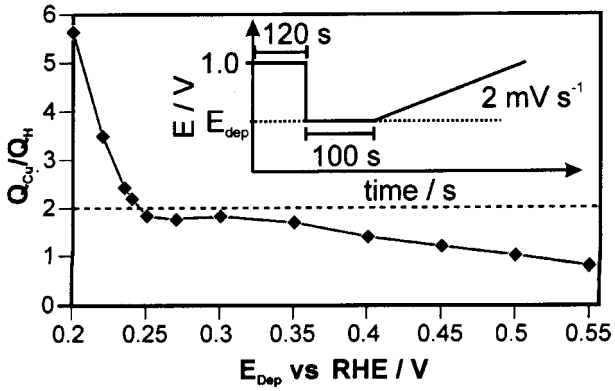

Figure 2. Ratio of copper stripping charge to hydrogen adsorption charge as a function of adsorption potential on a Pt polycrystalline electrode in a solution of 0.1 mol dm^{-3} H_2SO_4 and 0.5×10^{-3} mol dm^{-3} $CuSO_4$ polarized at various potentials for 100 s in the above solution. The charge associated with the copper stripping process was calculated by integrating the current obtained upon scanning the potential from the deposition potential to 1.0 V (RHE) at $\nu = 0.002$ V s^{-1} and correcting for the charge due to oxide growth observed in a solution free of $CuSO_4$.

for the upd of copper on platinum.[27] They saw several stripping peaks, with the weakest interaction occurring at around 0.25 V vs NHE. In agreement with them, we see that the deposition of upd copper, II_C, is shifted to much more positive potentials compared to the deposition of bulk copper and that the upd process results in the formation of four distinct peaks within the platinum double-layer region, indicating copper sites of different adsorption energies.

In Figure 2 is a plot of the ratio of the relative upd copper stripping charge (Q_{Cu}/Q_H) associated with copper deposited onto the planar polycrystalline platinum electrode as a function of deposition potential in a solution of 0.1 mol dm^{-3} H_2SO_4 and 0.5×10^{-3} mol dm^{-3} $CuSO_4$. Q_{Cu} is the charge obtained by integrating the copper upd stripping peaks, corrected for the background platinum electrochemistry. Q_H is the hydrogen charge on the same electrode in the absence of copper species in solution. Thus, this ratio is expected to be 2 under conditions in which a copper atom adsorbs on the platinum surface at the same sites and with the same surface density as the hydrogen

atoms. Our purpose in performing this experiment is to determine whether, for this concentration of copper in solution, it is possible to form a well-ordered layer of upd copper without the possibility of three-dimensional growth of bulk copper.[21] The platinum electrode was prepared so that it had no copper on its surface by prepolarizing it at 1.00 V for 120 s; the potential was then stepped to the deposition potential of interest, E_{dep}, for 100 s during which time the copper would deposit on the platinum surface. After this period had elapsed, the potential was scanned at 0.002 V s^{-1} up to a potential of 1.00 V in order to strip off the deposited copper, and the resulting stripping charge was used to construct the diagram. It is clearly evident that, below 0.25 V, deposition of bulk copper occurs, as might be expected from the reversible potential of the Cu/Cu^{2+} system, which is 0.242 V (RHE) in 0.5×10^{-3} mol dm^{-3} $CuSO_4$. Between 0.25 and 0.3 V, there is no change in deposition charge, and the ratio of the deposited charge to the hydrogen charge is close to 2, indicating that the upd layer completely forms over this potential range and that the coverage and surface density of the copper is the same as that for adsorbed hydrogen on the platinum surface (stripping of each copper atom produces two electrons compared to one for each hydrogen atom, hence the 2:1 ratio). Thus, we can be sure that, over this potential range, there is no contribution from the deposition of bulk copper. At potentials greater than 0.3 V, there is a loss in charge, as the upd layer is not fully formed. Similar results were obtained for ruthenium, in both cases indicating that a potential of 0.3 V allows for the complete formation of the upd layer while avoiding any deposition of bulk copper. This ensures that any deposits discussed are underpotential deposits alone.

The copper upd layer does not deposit instantly and might require some time to completely form. In Figure 3, we consider the amount of copper deposited as a function of polarization time at a deposition potential of 0.3 V. Both electrodes studied were prepolarized at 1.00 V for 120 s, and then the potential was stepped to 0.3 V. After a predetermined period, $t_{deposit}$, the copper deposited during that period was stripped off by applying a voltammetric ramp at 0.002 V s^{-1} up to a potential of 1.0 V. At short times, a significant increase in the height of peaks II_a in Figure 1 is seen (results not shown). As the polarization time is increased these peaks do not grow in concert with each other: the peaks at higher potential completely form first, and with successive increases in $t_{deposit}$, there is a growth in the upd peaks at lower potentials. This indicates that the rate of copper upd deposition depends on the adsorption sites. At longer times, the stripping voltammograms overlay each other, indicating that the deposition process has effectively finished. These results are condensed in Figure 3a for a planar platinum electrode and in Figure 3b for a high-surface-area Nafion-bound electrode. For both of these curves, the ratio Q_{Cu}/Q_H is plotted, as previously described for Figure 2. On the planar platinum electrode (Figure 3a), the upd layer is formed within about 30 s, with no further deposition of copper seen after this point. Similar results were obtained for ruthenium on titanium wire electrodes. The ratio of the copper upd stripping charge to the hydrogen charge is very close to 2, indicating that the copper atoms have the same coverage and surface density as electrochemically adsorbed hydrogen.

In the case of the high-surface-area platinum electrode (Figure 3b), slightly higher concentrations of copper in solution were required, although a monolayer was formed within 60 s of polarization of the electrode. Again, the ratio of the copper upd stripping to the hydrogen charge on this electrode is very close to 2. The higher concentration and longer period required for

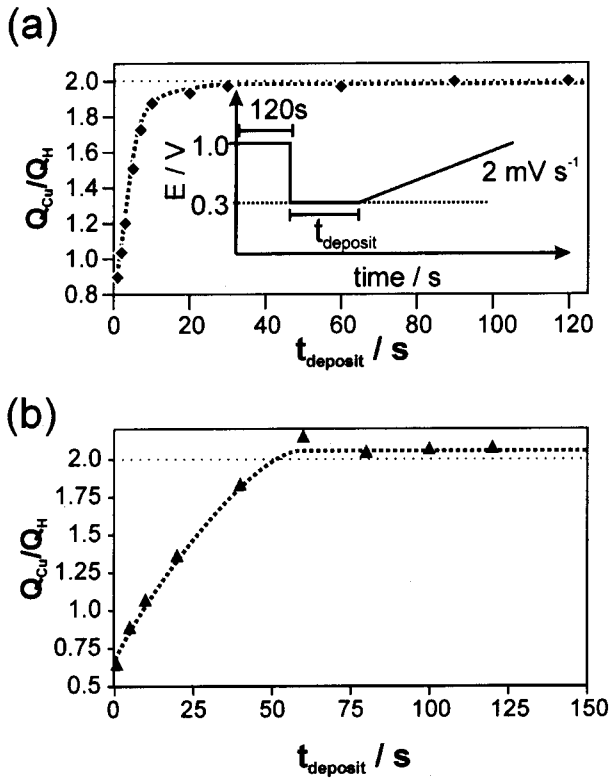

Figure 3. Ratio of copper stripping charge to hydrogen adsorption charge as a function of copper deposition time at 0.3 V (RHE) on (a) a Pt polycrystalline electrode and (b) a high-surface-area Nafion-bound electrode containing 0.5 mg cm^{-2} platinum. The solution contained 0.5 mol dm^{-3} H_2SO_4 and 0.5×10^{-3} mol dm^{-3} $CuSO_4$ for the former and 0.5 mol dm^{-3} H_2SO_4 and 2.0×10^{-3} mol dm^{-3} $CuSO_4$ for the latter experiment. The charge associated with the stripping process was calculated by integrating the current obtained on scanning the potential from 0.3 to 1.0 V (RHE) at $\nu = 0.002$ V s^{-1} and correcting for the background current in the absence of dissolved cupric ions.

the formation of the upd monolayer is undoubtedly due to diffusional limitations in the mass transport of cupric ions to the high-surface-area electrode surface. In subsequent experiments on high-surface-area electrodes, we used a cupric ion concentration of 0.002 mol dm^{-3} and a polarization time of at least 60 s. For higher precious-metal loadings or more highly dispersed catalysts than those used in this paper, it might very well be necessary to increase this adsorption time.

(b) Underpotential Deposition of Copper onto Planar Pt and Ru Bulk Electrodes. The underpotential deposition of copper onto polycrystalline platinum substrates has been extensively studied and used as a direct measure of electrochemical surface area by some workers.[28] Curve ii of Figure 4a shows a typical cyclic voltammogram for polycrystalline Pt in 0.1 mol dm^{-3} H_2SO_4 following potential cycling between the limits of oxygen and hydrogen evolution. The oxide formation and reduction and hydrogen adsorption and desorption regions are well-defined. The corresponding voltammogram in a mixture of 0.1 mol dm^{-3} H_2SO_4 and 5×10^{-4} mol dm^{-3} $CuSO_4$ following polarization at 0.3 V for 100 s is given in curve i of Figure 3a. On the forward and reverse sweeps, the stripping and adsorption of the upd copper film is seen.

The symmetry about the line of zero current nicely illustrates both the stripping and deposition processes, with higher symmetry achieved at slower scan rates. The charges associated with the deposition and stripping of copper, corrected for the background, were found to be approximately equal with a slight anodic excess. Such a discrepancy might well be expected be-

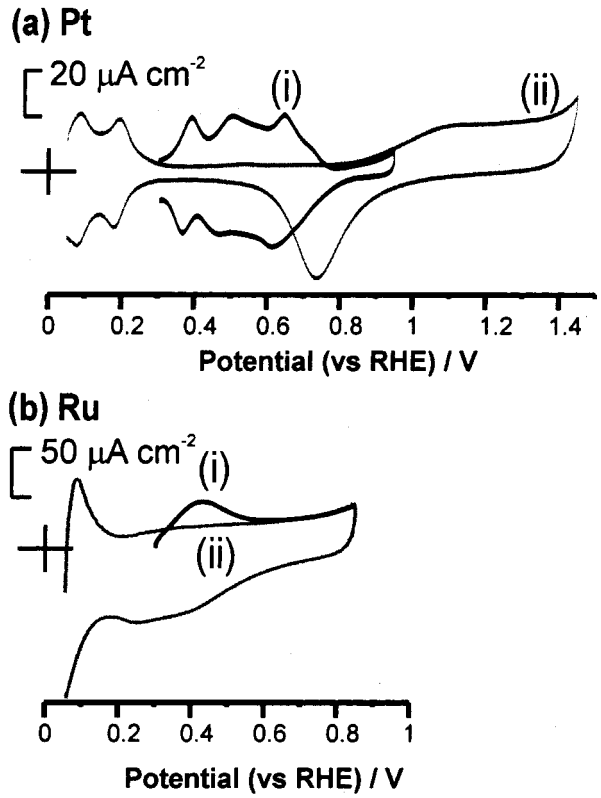

Figure 4. Copper upd in 0.1 mol dm^{-3} H_2SO_4 in the (i) presence and (ii) absence of 0.5×10^{-3} mol dm^{-3} $CuSO_4$ on bulk (a) platinum and (b) ruthenium electrodes. For i, the electrodes were polarized at 0.3 V for 100 s to form the upd layer, and the potential was then swept to 0.95 V and, in the case of platinum, back to 0.3 V. $\nu = 0.01$ V s^{-1}

TABLE 1: Hydrogen Adsorption and upd Copper Stripping Charge for a Polycrystalline 7-mm-Diameter Platinum Electrode

	charge (mC)	surface area (cm^2)
H adsorption	0.1296	0.617
Cu stripping	0.2595	0.633

cause of the lack of time allowed for the formation of the upd deposit during the scan in the cathodic direction, in agreement with the results presented in Figure 3.

Assuming that the hydrogen deposited in the hydrogen adsorption region corresponds to a monolayer coverage of hydrogen atoms, the coverage of an underpotential-deposited layer of copper can be found by comparing the charge due to the hydrogen monolayer with the charge associated with upd copper stripping. For the polycrystalline platinum disk electrode, the charges and associated surface areas are given in Table 1. From these values, the calculated coverage of copper is found to be very close to 1 ML. Markovich et al. found a maximum of ~0.9 ML coverage of copper on a Pt(111) disk[29] at a lower copper concentration than we have used (5×10^{-5} mol dm^{-3}) and in the presence of 10^{-2} mol dm^{-3} Cl^-. The agreement in coverages and surface areas calculated from H and Cu stripping indicate the reliability of the Cu upd technique in determining the electrochemical surface area of polycrystalline Pt electrodes.

It has been found that the maximum coverage of upd Cu on an electrodeposited Ru electrode is established at about 0.15−0.2 V vs NHE in $(1-5) \times 10^{-6}$ mol dm^{-3} $CuSO_4$ solution.[30] In contrast, we find good agreement for the deposition of Cu from the same solutions as used for the platinum electrode above and in the same potential range as mentioned previously for platinum. Displayed in Figure 4b are the results of a set of experiments similar to those already performed on platinum but carried out on a ruthenium electrode produced by electroless plating of ruthenium onto a titanium wire. The background scan (curve ii of Figure 4b) of the ruthenium electrode in 0.1 mol dm^{-3} H_2SO_4 shows significant differences from that seen on platinum. Oxidation of the ruthenium metal occurs at a much lower potential and is much broader and less structured than that of platinum. The ruthenium oxide produced is reduced on the reverse sweep starting at about 0.6 V, although the reduction peak is very broad and continues into the hydrogen adsorption region. Atomic hydrogen is produced at low potentials and is oxidized on the forward sweep. Copper also forms a upd layer on ruthenium. In a solution composed of 0.1 mol dm^{-3} H_2SO_4 and 5×10^{-4} mol dm^{-3} $CuSO_4$, a monolayer of copper is formed on the ruthenium if it is polarized at a potential of 0.3 V for 60 s or longer. Curve i of Figure 4b shows the linear sweep voltammogram for the stripping of this layer from the underlying ruthenium layer. Only one broad peak is seen, with its peak potential occurring at 0.4 V. This potential is close to the potential at which the stripping voltammogram of copper on platinum shows a trough (curve i of Figure 4a). Polarization at potentials below the reversible potential for the Cu/Cu^{2+} couple result in an additional peak or shoulder on the lower potential side of the upd peak whose size increases with time, confirming that this second peak is due to bulk deposition (results not shown).

(c) Surface Area Determination of Dispersed Pt, Ru, and Pt−Ru Electrodes Using CO Adsorption and Stripping. High-surface-area electrodes using unsupported platinum, ruthenium, and platinum−ruthenium powders were produced on glassy carbon electrodes using Nafion as the binder. Although we can use hydrogen adsorption to determine the surface area of electrodes composed of dispersed platinum, this approach cannot be used for electrodes composed of ruthenium or platinum−ruthenium. We have thus measured the surface area of the dispersed electrodes using CO stripping experiments and then used these electrodes in the study of the upd process on dispersed catalyst systems below. Results for the voltammetry of Nafion-bound platinum, ruthenium, and platinum−ruthenium electrodes in the absence and presence of an adsorbed layer of carbon monoxide are shown in Figure 5.

Curve ii of Figure 5a shows the voltammogram for the dispersed platinum electrode in 0.1 mol dm^{-3} H_2SO_4. The response is as would be expected for such an electrode and will not be discussed further. The background cyclic voltammogram for ruthenium in 0.1 mol dm^{-3} H_2SO_4 is shown in curve ii of Figure 5b and is typical for ruthenium electrodes[10] following potential cycling between 0.05 and 1.05 V. The voltammogram is comparable to that seen on the planar electrode in Figure 4b. This potential range has been used previously for such electrodes, and no dissolution of the Ru into H_2SO_4 was found. Surface oxidation occurs at low potentials overlapping with the peak at 0.1 V for hydrogen desorption/oxidation. Oxide reduction also occurs over a wide potential range, culminating in a peak at 0.2 V just prior to entering the region of H adsorption.

The cyclic voltammogram of dispersed platinum−ruthenium (curve ii of Figure 5c) shows features intermediate between those of ruthenium and platinum. Compared with ruthenium alone, the hydrogen adsorption/desorption regions are better defined and not masked to the same extent by the oxide formation and reduction peaks seen on pure ruthenium electrodes. The oxide reduction peak occurs at potentials negative of those for platinum but positive of those for ruthenium. The oxide reduction peak is broadened compared to those of both platinum and ruthenium.

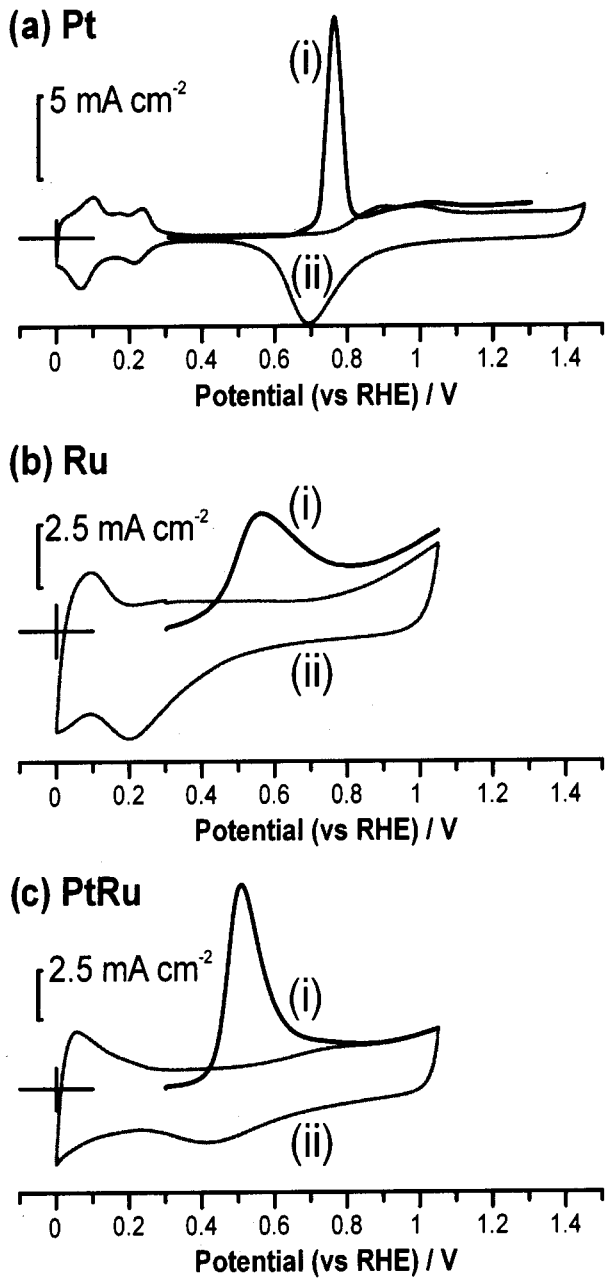

Figure 5. (i) Linear sweep stripping voltammogram for a monolayer of adsorbed CO and (ii) cyclic voltammogram in the absence of any CO for high-surface-area unsupported catalysts bound to a glassy carbon electrode with Nafion in a solution of 0.1 mol dm^{-3} H_2SO_4. The compositions and loadings of the electrodes are (a) 0.51 mg cm^{-2} platinum, (b) 0.43 mg cm^{-2} ruthenium, and (c) 0.51 mg cm^{-2} platinum−ruthenium, (c). $\nu = 0.01$ V s^{-1}.

Also shown are the voltammograms in the presence of an adsorbed layer of carbon monoxide. The different peak potentials for the stripping of a monolayer of carbon monoxide can clearly be seen. The peak potential for Pt (curve i of Figure 5a) occurs at 0.77 V, that for Ru (curve i of Figure 5b) at about 0.55 V on a broad peak, and that for Pt−Ru (curve i of Figure 5c) lower still at 0.50 V. These results reflect the combination of facile water dissociation on Ru and CO oxidation on Pt and are in agreement with the more extensive studies of this process.[12,13]

The corresponding surface areas are calculated assuming a 1:1 ratio of CO to each metal site (i.e., 420 μC cm^{-2}) and are provided in Table 2. Good agreement between the BET value for Pt and the corresponding values from CO stripping is found. The area that is calculated for the ruthenium electrode using CO stripping is around twice as large as that determined by the BET method. We can only assume that this discrepancy is possibly due to the assumption of a 1:1 stoichiometry between CO and surface ruthenium sites.

TABLE 2: Surface Area (m^2 g^{-1}) of Dispersed Powders Determined Using Different Methods

	measurement method			
	N_2 BET[a]	H adsorption	CO stripping	Cu stripping
Pt	50	53	52	55
Ru	15−25	NA	47	23
Pt−Ru	70−80	NA	69	74

[a] Information provided by manufacturer.

For mixed Pt−Ru alloys, a single metal−CO IR stretching frequency has been observed as a result of vibrational coupling between identical M−CO states on adjacent atoms, indicating that all CO is adsorbed in the same way.[31] There is, however, a dependence on the preparation method, and the mode of CO adsorption cannot be assumed to be identical on each atom. When distinct Pt and Ru clusters are present, at least two vibrational frequencies are found. If a mixture of bridge and linear bonds is present, then the situation is not clear-cut, and a single conversion value cannot be used for calculation of the surface area. The disagreement with the literature surface area values suggests that this is indeed the case.

It is for this reason that an alternative probe of surface area is sought. A method is required that can reliably give the surface area of mixed alloys irrespective of the preparation method and surface composition.

(d) Underpotential Deposition of Cu on High-Surface-Area Nafion-Bound Pt, Ru, and Pt−Ru. At a potential of 0.3 V, a monolayer of copper can be deposited not only on platinum but also on ruthenium and platinum−ruthenium electrodes. It was found that slightly increasing the concentration of copper in the solution to 0.002 mol dm^{-3} produced upd deposits more rapidly while still avoiding the possibility of bulk copper formation. Figure 6 shows stripping voltammograms for copper deposited from a solution of 0.1 mol dm^{-3} H_2SO_4 and 0.002 mol dm^{-3} $CuSO_4$ onto high-surface-area Pt, Ru, and Pt−Ru electrodes. These electrodes are the same as used for the experiments shown in Figure 5, and so, these results are directly comparable. These electrodes used a thin layer of Nafion to promote adhesion between the metal black and the glassy carbon substrate. In each case, the electrode was reduced in a solution containing no copper at a potential of 0.15 V before measurements were performed in the copper-containing solution. The electrode was then transferred into the copper-containing solution, and the upd film was formed by holding the potential at 0.3 V for 60 s. The copper was then removed from the surface during a positive sweep at 0.010 V s^{-1}.

The results obtained for a high-surface-area platinum electrode are shown in Figure 6a. The peaks obtained during stripping of the copper from the electrode surface (curve i of Figure 6a) show detail similar to that seen for the planar platinum electrode (Figure 4a). The small difference in peak shape and position might be due to the predominance of different crystal facets in the highly dispersed catalyst material compared to the polycrystalline planar electrode. For instance, it is known that small platinum particles tend to have a cubooctahedral geometry with a predominance of (100) and (111) crystal faces.[32,33]

The results of the experiment for copper deposited on Ru black are shown in Figure 6b. Curve i of Figure 6b shows the copper stripping experiment that involved polarization at 0.3 V for 60 s and then a positive sweep at 0.010 V s^{-1}. The stripping

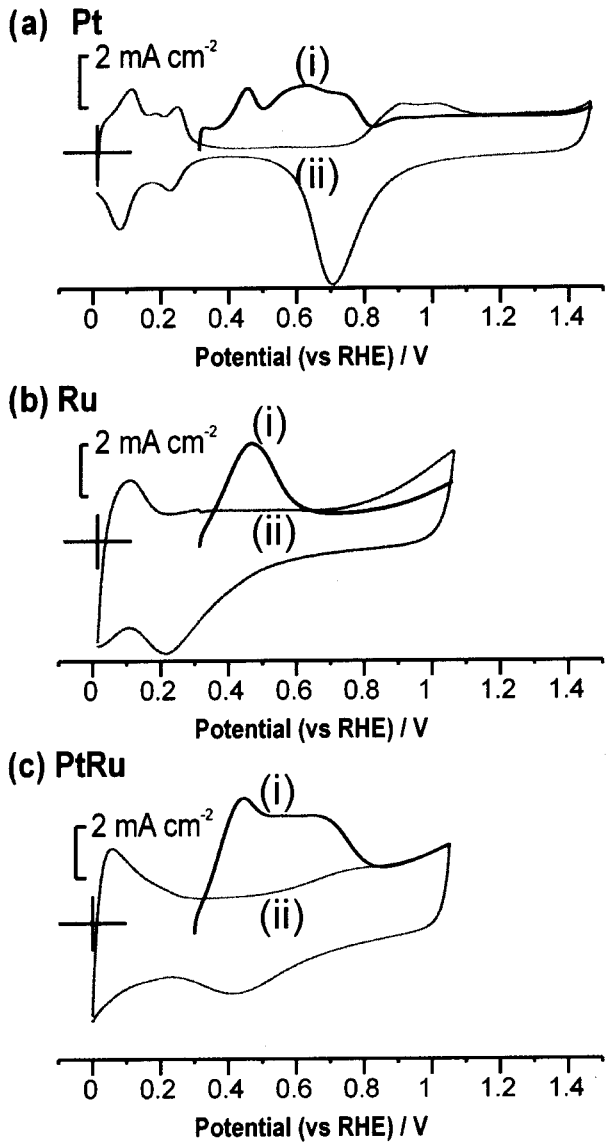

Figure 6. Background and upd stripping voltammetry for copper deposited onto high-surface-area unsupported catalysts bound to a glassy carbon electrode with Nafion: (a) 0.51 mg cm^{-2} platinum, (b) 0.43 mg cm^{-2} ruthenium, and (c) 0.51 mg cm^{-2} platinum−ruthenium. The upd stripping curves (i) were obtained in a solution composed of 0.1 mol dm^{-3} H_2SO_4 and 2×10^{-3} mol dm^{-3} $CuSO_4$, with the copper was adsorbed at 0.3 V for 60 s. Background scans (ii) were performed in 0.1 mol dm^{-3} H_2SO_4. In all cases, $\nu = 0.01$ V s^{-1}.

voltammetry of the copper upd layer is quite similar to that seen on the planar electrode and is, if anything, slightly clearer and better defined. Copper is removed from Ru electrodes at potentials marginally lower than the first stripping peak from Pt electrodes and significantly lower than the majority of the deposit from Pt. The peak potential for removal of the copper is centered at 0.45 V, slightly higher than seen for the planar ruthenium electrode (curve i of Figure 4b). In their study of electrodeposited ruthenium electrodes, Quiroz et al. noted that the potentials of bulk and upd deposition tend to coincide for electrodes with roughness factors greater than 30.[30] Surprisingly, even though our electrodes have roughness factors of several hundred, we do not see this effect, and the bulk and upd regions remain well separated. Two aspects of our electrode construction might account for this. The first is that we reduced our ruthenium electrodes under hydrogen to ensure that no chemically produced oxides (that cannot be electrochemically reduced) were present. The second is that the use of a Nafion sealant layer might stabilize the dispersion and reduce the extent of anion adsorption on the dispersed ruthenium. This might enhance the separation of the upd process from the bulk process.

Stripping of the upd layer formed on dispersed platinum−ruthenium is shown in curve i of Figure 6c. A peak at low potential is accompanied by a shoulder that continues to much higher potential. The similarity between the peak at low potential and that seen for copper upd on pure ruthenium (curve i of Figure 6b) is not coincidental but is, as will be shown below, directly due to copper deposition on ruthenium sites. The shoulder at higher potentials, which has its analogue in the response seen on platinum, is then due to the deposition of copper onto the platinum sites in the alloy catalyst.

Calculations of the surface areas of these electrodes were carried out by integrating the current voltage curve, corrected for the background current, and using a conversion factor of 420 μC cm^{-2}. In Table 2, the surface area values calculated by different means are reported to illustrate the applicability of the various techniques discussed herein to calculations of the surface area of the mixed alloy.

The values for Pt and Ru are in reasonable agreement with the BET surface areas, thus reflecting the reliability of all three electrochemical techniques in determining the true surface area. The one exception is the CO stripping measurement on Ru, which has been previously discussed. The value for Pt−Ru calculated from copper upd is in close agreement with the BET figure and the value from CO stripping. Because of the size similarities discussed earlier, the ratios of Cu to Pt and to Ru are 1:1. This permits a simple calculation of the total electrochemically active surface area for all three electrodes. The values obtained agree surprisingly well with both BET and hydrogen adsorption measurements (where applicable). This confirms the suitability of the copper upd process for measurement of surface areas for both elemental and unsupported high-surface-area alloy electrocatalysts. The potential problems with the CO adsorption method are illustrated for the case of CO adsorption on ruthenium for which the assumed 1:1 stoichiometry produces a surface area value more than twice as large as the BET measurement. In contrast, the copper upd measurement produces a value much closer to that determined through the BET method.

(e) Effect of Ruthenium Surface State on the Copper upd Process. The effect of oxide growth on the underpotential deposition of Cu on high-surface-area ruthenium is illustrated in Figure 7. A Nafion-bound high-surface-area ruthenium electrode was cycled in 0.1 mol dm^{-3} H_2SO_4 between 0.05 and 1.05 V at 0.01 V s^{-1} with the potential scan ending on the positive-going sweep at 0.05 V. The purpose of this initial treatment was to produce a surface on which virtually all of the ruthenium was in the reduced state. The potential was then stepped to various pretreatment potentials for 100 s during which time the surface oxidized to varying extents. The solution was then replaced with one containing 0.1 mol dm^{-3} H_2SO_4 and 2×10^{-3} mol dm^{-3} $CuSO_4$, after which the electrode was polarized at 0.3 V for 60 s. At the end of that time, the potential was scanned to 0.7 V at 0.01 V s^{-1}, producing plots b−d.

For the case when the pretreatment potential was 0.3 V (Figure 7b), very little oxide growth is expected, and the electrode surface is considered to be almost fully reduced. At higher potentials, progressively more oxide growth is expected, covering the surface and reducing the coverage of metallic ruthenium on which the copper upd process occurs. In agreement with other workers,[30] we found that the amount of upd copper decreases with increased growth of surface oxide. When the

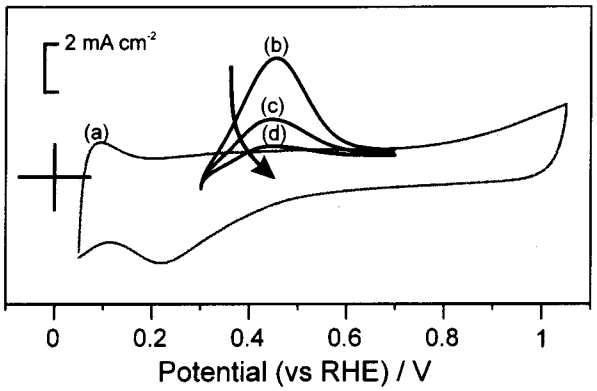

Figure 7. Background and upd stripping voltammetry for copper deposited onto high-surface-area unsupported 0.43 mg cm^{-2} ruthenium catalyst bound to a glassy carbon electrode with Nafion. (a) Background response in 0.1 mol dm^{-3} H_2SO_4 and stripping voltammetry as a function of pretreatment potential (300 s) at (b) 0.3, (c) 0.5, and (d) 1.05 V. The copper was adsorbed at 0.3 V for 60 s from a solution composed of 0.1 mol dm^{-3} H_2SO_4 and 2×10^{-3} mol dm^{-3} $CuSO_4$ at $\nu = 0.01$ V s^{-1}.

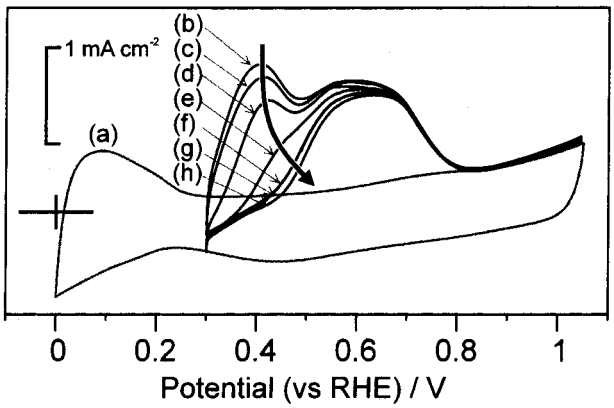

Figure 8. Background and upd stripping voltammetry for copper deposited onto high-surface-area unsupported 0.51 mg cm^{-2} platinum−ruthenium catalyst bound to a glassy carbon electrode with Nafion. (a) Background response in 0.1 mol dm^{-3} H_2SO_4 and stripping voltammetry as a function of pretreatment potential (300 s) at (b) 0.3, (c) 0.45, (d) 0.55, (e) 0.65, (f) 0.75, (g) 0.85, and (h) 0.95 V. The copper was adsorbed at 0.3 V for 60 s from a solution of 0.1 mol dm^{-3} H_2SO_4 and 2×10^{-3} mol dm^{-3} $CuSO_4$ at $\nu = 0.01$ V s^{-1}.

pretreatment potential is 0.5 V (Figure 7c), a significant reduction in the amount of copper deposited occurs. A further increase of the pretreatment potential to 1.05 V (Figure 7d) suggests that virtually no copper has been deposited on the surface. It would appear that Cu upd can be used as a sensitive probe for determining the amount of bare ruthenium sites present on the surface of the electrode.

A similar effect is not seen for platinum electrodes, as platinum oxides are completely reduced at potentials much higher than the copper deposition potentials used. Although it is recognized that the potential required for the reduction of Cu^{2+} also coincides with that for the reduction of ruthenium oxides, the much-reduced stripping peaks for the higher coverages of oxide suggest that reduction in the presence of copper is minimal. On ruthenium, the formation of RuO_x is highly, although not completely, irreversible.[34] Oxide formed in the range of 0.61−1.01 V substantially remains on the electrode surface following polarization for copper deposition at 0.3 V.

In our work, all ruthenium metallic surface area could be recovered following reduction of the electrode surface by polarization at low potentials (0.25 V) or by potential cycling between 0 and 1.05 V with the scan ending at the low potential, both in copper-free solutions.

(f) Effect of Platinum−Ruthenium Surface State on the Copper upd Process. Although no effect is seen on the copper upd process for high-surface-area platinum electrodes polarized at higher potentials, such effects are seen on high-surface-area platinum−ruthenium electrodes. Figure 8a shows the current voltage curves for a Pt−Ru/Nafion/GC electrode in 0.1 mol dm^{-3} H_2SO_4. As for the case with ruthenium discussed above, the electrode was precycled in 0.1 mol dm^{-3} H_2SO_4 between 0 and 1.05 V with the potential stopped at the lower limit. The potential was then stepped to various pretreatment potentials for 300 s and then to 0.3 V. The solution was replaced with one composed of 0.1 mol dm^{-3} H_2SO_4 and 2×10^{-3} mol dm^{-3} $CuSO_4$, and the electrode was polarized at 0.3 V for 60 s. The background voltammogram can be recovered upon potential cycling in a copper-free solution following each subsequent oxide formation step, indicating no dissolution of ruthenium ions (as discussed later).

Figure 8b shows the underpotential deposition of copper on a fully reduced high-surface-area Pt−Ru catalyst. As previously seen in Figure 6c, stripping of the copper upd on Pt−Ru results in two distinctive peaks. The narrower one at around 0.38 V is followed by a broad peak centered at 0.6 V. The first peak occurs at a potential similar to that found on the Ru electrodes. From a comparison with the stripping voltammograms for Pt and Ru alone (Figure 6a and b), the peaks are assigned as follows. The first peak is due to stripping of the deposit from surface ruthenium sites, although a small contribution will arise from Pt (discussed later), and the second, broader peak reflects removal from Pt sites only. The copper upd stripping peaks at higher potentials remain relatively unchanged as the prepolarization potential is increased.

Increasing the amount of surface oxide by polarization at progressively higher potentials decreases the size of the first peak. The polarization potentials chosen are lower than those required to induce oxidation of platinum, and so, the decrease is attributed to the formation of ruthenium oxides only.

From Figure 8b-h the amount of surface ruthenium in the reduced electrode can be calculated assuming that the loss in copper upd is entirely due to oxidation of the surface ruthenium to its oxide. The total charge under the copper upd peak for the fully reduced electrode (Figure 8b) is assumed to represent the entire metal surface, i.e., the total platinum and ruthenium metal surface, and the extent of ruthenium oxide at this electrode is assumed to be negligible. As has been shown previously, this surface area correlates well with the surface area calculated using CO adsorption and stripping. Polarization at successively higher potentials will result in the formation of progressively more surface oxide, and as a result, there will be a decrease in the size of the first peak and a decrease in the total charge. At a high potential of 0.95 V (Figure 8h), virtually all of the ruthenium is in its oxidized state, and we assume that the surface is composed of ruthenium with a surface oxide and metallic platinum. Thus, for electrodes pretreated at this potential, the observed copper upd response is solely due to the platinum surface area of the catalysts. Utilizing this measured platinum surface area, it is possible to calculate the coverage of bare ruthenium sites as a function of the prepolarization potential.

Before doing so, however, it is useful to question whether the polarization regime used above results in a truly steady-state system or whether oxide formation at the potentials used in the above experiments would be expected to be incomplete after the 300-s polarization period used. Polarization of a high-

surface-area Pt−Ru electrode previously reduced at 0.145 V for 500 s results in a current transient that shows a significant tail. This transient is due to the growth of ruthenium oxide on the surface. Figure 9 provides two representative transients taken for potential steps to 0.645 and 0.745 V for an electrode containing 60 μg of catalyst in 0.5 mol dm^{-3} sulfuric acid. The figure shows the natural logarithm of the current as a function of time. At longer times (i.e., $t > 100$ s), the current decays exponentially, as seen by the linear section of the graph, with the transient at 0.745 V decaying at a slower rate than that at 0.645 V. Furthermore, the current becomes quite noisy at longer times for the latter transient as the measured currents approach the minimum values that can be resolved by our potentiostat during this experiment. Regression of the linearized form of the current transient, as presented in Figure 9 for the response at times greater than 100 s, produces a very good fit, as seen from the dashed lines in Figure 9. At times less than 100 s, the currents are larger than expected from the exponential decay. We can now calculate whether 300 s is long enough to fully form the equilibrium oxide coverage on our platinum−ruthenium electrode.

We consider that the current that flows is the sum of two different components: the exponentially decaying current, representative of the slow oxide growth process that dominates at long times (i.e., $t > 100$ s), i_{exp}, and the excess current seen at short times due to double-layer charging and some of the oxide growth processes, i_{init}

$$i = i_{init} + i_{exp} \tag{7}$$

As i_{init} becomes insubstantial at times longer than 100 s, we can use the integrated form of the exponential, which we fitted to the current decay to determine the total extra charge expected for growth of the oxide were the experiment continued indefinitely, Q_{exp}. Combining this charge with the excess charge seen at short times, Q_{init}, we can calculate the total charge expected to flow in order to produce the equilibrium oxide coating, Q_∞

$$Q_\infty = Q_{init} + Q_{exp} = \int_0^\infty i_{init}\,dt + \int_0^\infty i_{exp}\,dt = \int_0^{500} i\,dt + \int_{500}^\infty i_{exp}\,dt \tag{8}$$

$$= \int_{500}^\infty i\,dt + \frac{-\exp(500a + b)}{a}$$

where a and b are the fitting parameters for the exponential current decay [$i_{exp} = \exp(at + b)$], with a necessarily being negative for a current decay. The first component of Q_∞ can be determined from the experimental data, and the second component can be determined from the fitting parameters of the exponential current decay. Table 3 provides calculated Q_∞ values for potentials ranging from 0.645 to 0.945 V, along with the experimentally measured total charges passed 300 and 500 s into the chronoamperometric experiment. At 300 s, the extent of completion of formation of the equilibrium oxide layer is seen to decrease with increasing potential; nevertheless, at the highest potential studied, the oxide layer is still 85% complete. Thus, we can be assured that the oxide film is almost totally formed after 300 s of polarization, with some deviation being seen at the highest potentials. For comparison, chronocoulombetric plots for the data presented in the main body of Figure 9 are provided in the inset to that figure. The horizontal dashed lines represent the Q_∞ values calculated at each of these potentials.

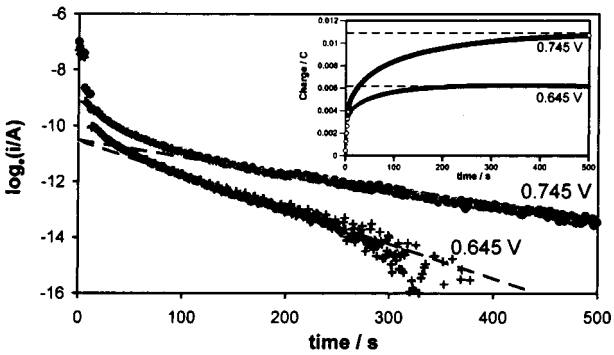

Figure 9. Logarithmic current transients during the polarization of high-surface-area unsupported 0.212 mg cm^{-2} platinum−ruthenium catalyst bound to a 3-mm-diameter glassy carbon electrode with Nafion in 0.5 mol dm^{-3} H_2SO_4. The electrode was polarized at 0.145 V for 500 s before polarization at 0.645 and 0.745 V. The dashed lines represent a fit to the linear part of the transient at times >100 s. Inset: Chronocoulombetric plots for the current transients in the main diagram. The dashed lines represent the limiting total charge for polarization of the electrodes; see text for description.

TABLE 3: Extent of Oxide Growth on Unsupported Pt−Ru in 0.5 Mol dm^{-3} H_2SO_4 as a Function of Polarization Potential and Time

				extent of completion of oxide growth		
E (RHE) (V)	Q_{300} (mC)	Q_{500} (mC)	Q_∞ (mC)	after 300 s	after 500 s	θ_∞[a]
0.645	6.2	6.2	6.2	100%	100%	0.35
0.745	10.2	10.7	10.9	93%	98%	0.62
0.845	12.0	13.0	13.6	88%	95%	0.77
0.945	14.8	16.2	17.5	85%	93%	0.99

[a] Extent of total equilibrium oxide coverage using BET surface area of catalyst (Table 2) and assuming two electrons per surface site.

Also, in the last column of Table 3 is the ratio of the Q_∞ charge to the charge required to form a monolayer on the Pt−Ru catalyst assuming that two electrons are transferred per surface site (i.e., 420 μC cm^{-2}). The charges passed are a significant fraction of a monolayer and, at the highest potential studied, approach the charge expected for a complete monolayer of adsorbed oxygen. Over the potential range studied, the growth of oxide is expected to be almost entirely on the ruthenium component of the catalyst. However, as the charge measured is close to one monolayer on the *entire* catalyst surface, there must be a significant component of multilayer ruthenium oxide formation to this charge. As the extent of formation of such multilayer oxide is difficult to judge, it seems difficult to relate the Q_∞ values directly to the amount of unoxidized ruthenium on the catalyst surface.

In contrast, the copper stripping measurements provide a direct measure of the coverage of unoxidized ruthenium sites on the catalyst surface. The coverage of bare ruthenium sites, $\theta_{Ru,E_{pretreat}}$ on the platinum−ruthenium catalyst at a given potential, $E_{pretreat}$, can be calculated from the charge associated with copper upd stripping at that potential, $Q_{E_{pretreat}}$; the charge associated with copper upd stripping on the platinum component alone, Q_{Pt}; and the charge associated with copper upd on the fully reduced platinum−ruthenium catalyst, $Q_{Pt-Ru(red)}$

$$\theta_{Ru,E_{pretreat}} = \left(\frac{Q_{E_{pretreat}} - Q_{Pt}}{Q_{Pt-Ru(red)}}\right) \tag{9}$$

If we take Q_{Pt} to be the copper upd charge determined for the catalyst prepolarized at 0.95 V, and $Q_{Pt-Ru(red)}$ to be the

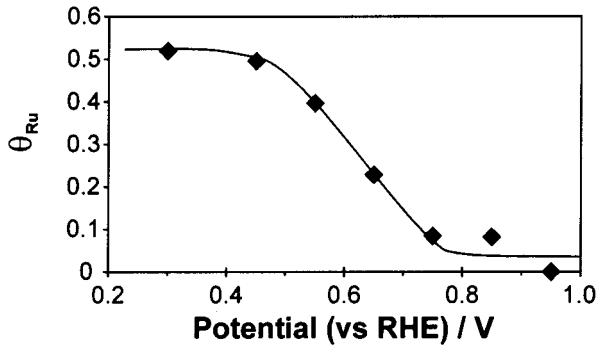

Figure 10. Variation of surface coverage of ruthenium metal as a function of polarization potential calculated from copper upd. Data obtained from Figure 8.

copper upd charge determined for the catalyst prepolarized at 0.3 V, then we can obtain a plot of the surface coverage of bare ruthenium sites as a function of potential as shown in Figure 10. A nonlinear relationship between the surface ruthenium metal and the oxidation potential is observed. The coverage for the reduced surface starts at the nominal value of 0.5 and does not appear to significantly change until the polarization potential exceeds 0.45 V, after which it undergoes a linear decline before leveling off at higher potentials at a value close to zero. Thus, over the potential range at which platinum−ruthenium catalysts are used in reformate-fed and direct methanol fuel cells (0−0.5 V), the majority of the ruthenium on the surface of the catalyst is in the zero-valent state. In a following paper, we will consider the effect of surface ruthenium oxidation state on the activity of platinum−ruthenium electrocatalysts toward methanol oxidation.[35]

This analysis of surface bare ruthenium site coverage relies on three assumptions. The first is that the use of copper upd on an electrochemically reduced surface provides a good measure of the *total* metal surface area (i.e., platinum plus ruthenium) and that there is no significant oxide growth at 0.3 V during formation of the copper upd film. The second is that, when the surface is polarized at 0.3 V to form the copper upd layer after having been polarized at higher potentials, no significant reduction of the ruthenium oxides produced at those higher potentials occurs. The final assumption is that the surface produced by polarizing the electrode at 0.95 V is effectively free of bare ruthenium sites, i.e., that the peak produced at 0.35 V during the copper stripping process on the reduced electrodes is due to copper upd onto ruthenium sites on the catalyst.

In support of the first assumption, it has been shown that the copper upd process shows surface areas that closely follow those seen with CO adsorption and stripping. Furthermore, the background voltammetry of ruthenium and platinum−ruthenium electrodes indicates that, although some growth of oxide might occur at these low potentials, the amount produced is quite small, and much larger potentials are required to form significant coverages of oxide on ruthenium. Thus, the discrepancy arising from formation of oxides during the copper upd process can be considered to be quite small.

As to the second assumption, the degree to which any oxide formed on the ruthenium in the platinum−ruthenium electrode is reduced during the copper upd process is, to a large extent, controlled by the reversibility of ruthenium oxide formation. This process is highly irreversible, with the majority of oxide not being reduced until below the 0.3 V potential at which the copper upd layer is formed. Furthermore, this process is quite sluggish and slow. Any artifact due to the reduction of oxide during the copper deposition process will be more serious for electrodes that have been polarized at high potentials, as such electrodes will have the largest oxide coverage and thus the greatest propensity to lose some of that oxide coverage via reduction. Independent experiments suggest that the extent of this reduction leads to an underestimate of oxide coverage by not more that 10−20% at the highest potential studied and a progressively smaller loss at lower potentials.

TABLE 4: Standard Potentials at Which Higher Oxides of Ruthenium Are Formed[31]

electrode reaction	standard potential (V)
$Ru^{3+} + e^- \rightarrow Ru^{2+}$	0.2487
$Ru^{2+} + 2e^- \rightarrow Ru$	0.455
$RuO_4 + 8H^+ + 8e^- \rightarrow Ru + 4H_2O$	1.038
$RuO_2 + 4H^+ + 2e^- \rightarrow Ru^{2+} + 2H_2O$	1.120
$RuO_4 + 6H^+ + 6e^- \rightarrow Ru(OH)_2^{2+} + 2H_2O$	1.4

Our third assumption is considered in the following section.

(g) Loss of Surface Bare Ruthenium Sites from Platinum−Ruthenium Catalysts by Oxidation at High Potentials. The assumption that the peak in the upd stripping curves at low potentials (0.35 V) is due to the adsorption of copper on ruthenium sites is in part borne out by the similarity of that peak to the peak seen in upd stripping on dispersed ruthenium electrodes (Figure 6b). Further evidence for this assignment comes from experiments in which we selectively remove ruthenium from the electrocatalyst surface by polarization of that electrode at high potentials. By polarizing the electrode above 1.05 V, i.e., into the platinum oxidation region, higher oxides of ruthenium can be formed. The standard potentials of these higher oxides are indicated in Table 4.

RuO_4 has previously been found to be a volatile corrosion product of Ru and RuO_2 oxidation at oxygen evolution potentials in acidic electrolyte. Detection was achieved via on-line mass spectrometry[36] and, more recently, by potential-modulated reflectance spectroscopy.[37]

To facilitate the removal of ruthenium from the dispersed Pt−Ru electrodes, we polarized them at 1.45 V in 0.1 mol dm^{-3} H_2SO_4 for 100 s with continuous agitation of the solution provided by argon bubbling. The Pt−Ru electrode was then cycled 10 times between 0 and 1.05 V. The sequence of polarization at high potential followed by potential cycling was carried out 12 times, and selected results of the final potential cycle are displayed in Figure 11. Several interesting features are illustrated. There is a decrease in the size of the Pt−Ru oxide reduction peak at 0.35 V (I_C) with cycle number. Concurrent with this decrease is the introduction and growth of a reduction peak at higher potentials (II_C). A decrease in the size of the broad oxide formation peak, I_A, is seen, as is an increase in the sharpness of the hydrogen oxidation region, II_A.

The development of peak II_C corresponds to the reduction of platinum oxides, indicating that oxidation of platinum was occurring, whereas the loss of charge from peak I_C suggests a decrease in the amount of active ruthenium oxide present on the electrode surface. Furthermore, the development of more defined peaks in the hydrogen adsorption/desorption region is also seen as a function of polarization at the higher potential limit. Indeed, from Figure 11, the final voltammogram obtained for the largest number of cycles is seen to show very similar features to those expected for a platinum electrode, admittedly with some distortion. Electrodes prepared in this way will be called ruthenium-depleted Pt−Ru electrodes. Reduction of a ruthenium-depleted electrode at 0 V for extended periods did not result in recovery of the platinum−ruthenium electrochemistry; indeed, there was no change in the voltammetry from that observed in the final scan of Figure 11.

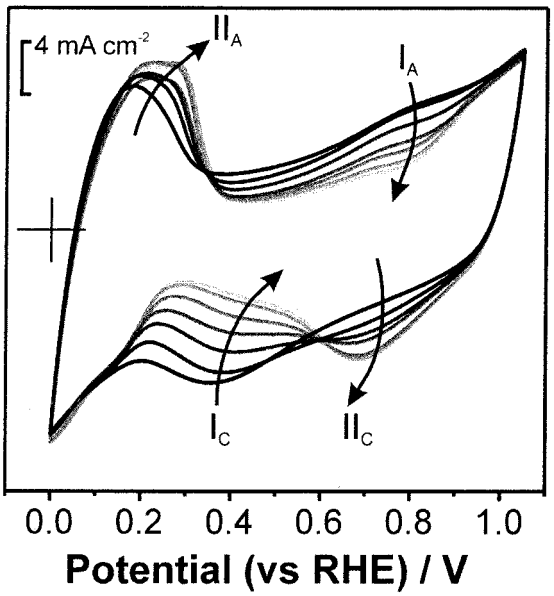

Figure 11. Cyclic voltammograms for a high-surface-area unsupported platinum−ruthenium catalyst (0.51 mg cm^{-2}) bound to a glassy carbon electrode with Nafion. Response in 0.1 mol dm^{-3} H_2SO_4 (a) following cycling to constant CV between 0 and 1.05 V and following the (b) 1st, (c) 3rd, (d) 5th, (e) 7th, (f) 9th, and (g) 11th cycles of polarization at 1.45 V for 300 s in stirred solution. $\nu = 0.05$ V s^{-1}.

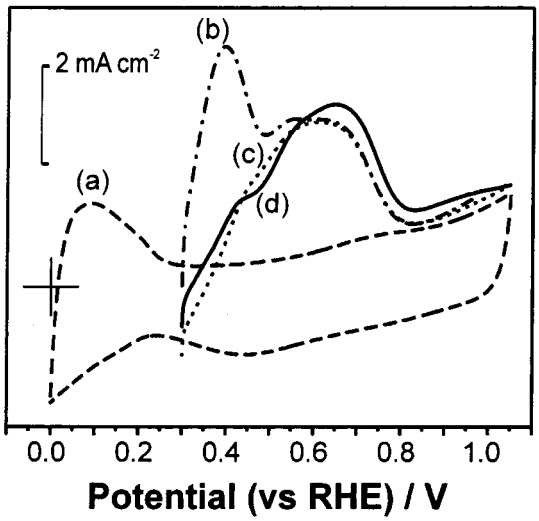

Figure 12. Background and upd stripping voltammetry for copper deposited onto high-surface-area unsupported 0.51 mg cm^{-2} platinum−ruthenium catalyst bound to a glassy carbon electrode with Nafion. (a) Background response in 0.1 mol dm^{-3} H_2SO_4, (− − −), (b) stripping voltammetry at fully reduced surface (−•−•−•), (c) following polarization at 1.05 V to leave fully oxidized surface (•••), and (d) following 100 potential cycles to 1.45 V at 10 mV/s (—). The copper was adsorbed at 0.3 V for 60 s from a solution of 0.1 mol dm^{-3} H_2SO_4 and 2×10^{-3} mol dm^{-3} $CuSO_4$ at $\nu = 0.01$ V s^{-1}.

It therefore seems reasonable that, at potentials of 1.45 V, an irreversible loss of bare ruthenium sites from the electrode surface occurs and that this leads to a surface rich in platinum. Depending on the ruthenium oxides present at these potentials, loss of ruthenium into solution might also occur through dissolution. No attempt has been made to detect such dissolution products. The Pourbaix diagram[38] for ruthenium suggests that, in strongly acidic solutions, ruthenium is passivated over the potential range 0.8 to 1.3 V and that, at potentials higher than this, corrosion and the formation of soluble RuO_4 occur. An alternative explanation for this effect is that, at higher potentials, place exchange of surface ruthenium for buried platinum in the alloy occurs, leading to an enrichment of the surface with platinum. This process would produce a catalyst with electrochemistry that looked essentially "platinum-like", although probably without any significant dissolution of ruthenium.

The effect of this surface treatment on the copper upd film produced on the electrode is explored in Figure 12 in which a comparison is made between the stripping curves on a reduced Pt−Ru electrode, an oxidized Pt−Ru electrode, and a reduced ruthenium-depleted electrode. On the reduced Pt−Ru electrode surface (Figure 12b), as expected there are two characteristic peaks, one at 0.35 V and the other broader peak at 0.6 V. As seen previously, the oxidized Pt−Ru surface produces a copper upd stripping voltammogram in which the first peak is lost (Figure 12c). The reduced ruthenium-depleted voltammogram (Figure 12d) shows a response very similar to that observed for the oxidized Pt−Ru surface, although there is an increase in the height of the peak at higher potentials, as well as the indication of a peak at about 0.42 V. This latter peak occurs at the same potential as the peak seen during the stripping of the copper upd layer on dispersed platinum (Figure 6a). Interestingly, although there is some increase in the platinum surface area, this increase does not match the area lost through the oxidation of the ruthenium. This suggests a loss in overall surface area of the electrode and might be caused by some degree of sintering of the catalyst particles or potentially through the formation of surface ruthenium oxides that are not electrochemically active, i.e., they simply act to block the surface and are not electrochemically reduced during the electrochemical pretreatment.

Thus, these results confirm the assignment of the copper upd peak at 0.4 V as being due to the deposition of copper on ruthenium sites.

Conclusions

In this paper, we have introduced a new method for measuring the surface area of highly dispersed platinum, ruthenium, and platinum−ruthenium catalysts and applied that method to the study of unsupported catalysts. In a following paper, we will examine the application of this method to the study of supported forms of these catalyst. The possibilities for wider use of the underpotential deposition of copper onto Pt, Ru, and Pt−Ru electrodes are vast. We have shown here that the stripping of the underpotential deposit of Cu can be used as an accurate probe of the electrochemically active surface areas of Pt and Ru and, most importantly, each of these metals in Pt−Ru electrodes. This is an improvement over the currently used method of CO monolayer stripping as, because of size similarities, it is safe to assume that the complete copper monolayer is deposited in a 1:1 manner on the substrate atoms regardless of the Pt/Ru ratio. The technique is simple to perform, being carried out in an aqueous environment under standard conditions, and significantly, it is nondestructive to electrodes. One must exercise caution however for its use on electrodes in fuel cell configurations, as soluble transition metals are well-known poisons in solid polymer fuel cells.[39]

In addition we have shown that Cu upd can be used to determine the coverage of bare ruthenium sites on the electrode surface. It is important to be able to determine the nature of the ruthenium within the Pt−Ru electrode, as unlike the platinum component, ruthenium oxides are not easily reduced electrochemically and so will persist on the electrode surface altering its electrocatalytic properties. By carrying out the upd experiment on an electrode taken directly from a fuel cell and

comparing the charges attained with those for the fully reduced electrode, the activity of the electrode can easily be correlated with the surface ruthenium composition and, as such, can provide an interesting picture of the ideal state of the electrode. An assessment of the activities of electrodes with different bare ruthenium site coverages (as opposed to *total* ruthenium coverages) and correlation with the activities of those electrodes toward the methanol oxidation reaction will be presented in a forthcoming paper.

Acknowledgment. One of us (C.G.) acknowledges financial support for a Quota studentship from the U.K. EPSRC. The authors thank Johnson Matthey Plc. for providing the high-surface-area catalyst samples.

References and Notes

(1) Toda, T.; Igarashi, H.; Watanabe, M. *J. Electroanal. Chem.* **1999**, *460*, 258.
(2) Watanabe, M.; Tsurumi, K.; Mizukami, T.; Nakamura, T.; Stonehart, J. *J. Electrochem. Soc.* **1994**, *141*, 2659.
(3) Wasmus, S.; Küver, A, *J. Electroanal. Chem.* **1999**, *461*, 14.
(4) Rolison, D. R.; Hagans, P. L.; Swider, K. E.; Long, J. W. *Langmuir* **1999**, *15*, 774.
(5) Long, J. W.; Stroud, R. M.; Swider-Lyons, K. E.; Rolison, D. R. *J. Phys. Chem. B* **2000**, *104*, 9772.
(6) Markovic, N. M.; Gasteiger, H. A.; Ross, P. N.; Jiang, X. D.; Villegas, I.; Weaver, M. J. *Electrochim. Acta* **1995**, *40*, 91.
(7) Lin, W. F.; Zei, M. S.; Esiwirth, M.; Ertl, G.; Iwasita, T.; Vielstich, W. *J. Phys. Chem. B* **1999**, *103*, 6968.
(8) Essalik, A.; Amouzegar, K.; Savagogo, O. *J. Appl. Electrochem.* **1995**, *25*, 404.
(9) Yamamoto, K.; Kolb, D. M.; Kotz, R.; Lehmpfuhl, G. *J. Electroanal. Chem.* **1979**, *96*, 233.
(10) Kinoshita, K.; Ross, P. N. *J. Electroanal. Chem.* **1977**, *78*, 313.
(11) Schmidt, T. J.; Noeske, M.; Gasteiger, H. A.; Behm, R. J.; Britz, P.; Brijoux, W.; Bonnemann, H. *Langmuir* **1997**, *13*, 2591.
(12) Gasteiger, H. A.; Markovic, N.; Ross, P. N.; Cairns, E. J. *J. Phys. Chem.* **1994**, *98*, 617.
(13) Dinh, N. H.; Ren, X.; Garzon, F. H.; Zelanay, P.; Gottesfeld, S. *J. Electroanal. Chem.* **2000**, *491*, 222.
(14) Kinoshita, K.; Ross, P. N. *J. Electroanal. Chem.* **1977**, *78*, 313.
(15) Miura, H.; Suzuki, H.; Ushikubo, Y.; Sugiyama, K.; Matsuda, T.; Gonzalez, R. D. *J. Catal.* **1984**, *85*, 331.
(16) Gasteiger, H. A.; Ross, P. N.; Cairns, E. J. *Surf. Sci.* **1993**, *293*, 67.
(17) Catttaneo, C.; Sanchez de Pinto, M. I.; Mishima, H.; Lopez de Mishima, B. A.; Lescano, D.; Cornaglia, L. *J. Electroanal. Chem.* **1999**, *461*, 32.
(18) Ross, P. N. *Electrochim. Acta* **1991**, *36*, 2053.
(19) Scortichini, C. L.; Reiley, C. N. *J. Electroanal. Chem.* **1982**, *139*, 233.
(20) Quiroz, M. A.; Meas, Y.; Lamy-Pitara, E.; Barbier, J. *J. Electroanal. Chem.* **1983**, *157*, 165.
(21) Ficicioglu, F.; Kadirgan, F. *J. Electroanal. Chem.* **1993**, *346*, 187.
(22) Lamy-Pitara, E.; Barbier, J. *Appl. Catal. A: Gen.* **1997**, *149*, 49.
(23) Kolb, D. M. *Adv. Electrochem. Electrochem. Eng.* **1978**, *11*, 25
(24) Kokkinidis, G. *J. Electroanal. Chem.* **1986**, *201*, 217.
(25) Trasatti, S.; Petrii, O. A. *J. Electroanal. Chem.* **1992**, *327*, 353.
(26) Machado, S. A. S.; Tanaka, A. A.; Gonzalez, E. R. *Electrochim. Acta* **1991**, *36*, 1325.
(27) Danilov, A. I.; Molodkina, E. B.; Polukarov, Y. M. *R. J. Electrochem.* **1998**, *34*, 1249.
(28) Elliott, J. M.; Birkin, P. R.; Bartlett, P. N.; Attard, G. S. *Langmuir* **1999**, *15*, 7411.
(29) Markoviæ, N. M.; Gasteiger, H. A.; Ross, P. N. *Langmuir* **1995**, *11*, 4098.
(30) Quiroz, M. A.; Gonzalez, I.; Vargas, H.; Meas, Y. E.; Lamy-Pitara, E.; Barbier, J. *Electrochim. Acta* **1986**, *31*, 503.
(31) Ianniello, R.; Schmidt, V.; Stimming, U.; Stumper, J.; Wallau, A. *Electrochim. Acta* **1994**, *39*, 1863.
(32) Giordano, N.; Passalacqua, E.; Pino, L.; Arrico, A. S.; Antonucci, V.; Vivaldi, M.; Kinoshita, K. *Electrochim. Acta* **1991**, *36*, 1979.
(33) Zubimendi, J. L.; Andreasen, G.; Triaca, W. E. *Electrochim. Acta* **1995**, *40*, 1305.
(34) Nguten Van Huong, C.; Gonzalez-Tejera, M. J. *J. Electroanal. Chem.* **1988**, *244*, 249.
(35) Green, C.; Kucernak, A., manuscript in preparation.
(36) Wohlfahrtmehrens, M.; Heitbaum, J. *J. Electroanal. Chem.* **1987**, *237*, 251.
(37) Walker, R. C.; Bailes, M.; Peter, L. M. *Electrochim. Acta* **1998**, *44*, 1289.
(38) De Zourbov, N.; Pourbaix, M. *Atlas of Electrochemical Equilibria in Aqueous Solution*; National Association of Corrosion Engineers: Houston, TX, 1966; Section 13.1.
(39) Andolfatto, F.; Durand, R.; Michas, A.; Millet, P.; Stevens, P. *Int. J. Hydrogen Energy* **1994**, *19* 421.